Multiple magnetic resonance of nuclei in a two-dimensional electron system

Xuan Qian,[1] Yang Ji,[1,*] and Vladimir Umansky[2]

[1]*SKLSM, Institute of Semiconductors, Chinese Academy of Sciences, Beijing 100083, People's Republic of China*

[2]*Department of Condensed Matter Physics, Braun Center for Submicron Research, Weizmann Institute of Science, Rehovot 76100, Israel*

(Received 24 June 2015; revised manuscript received 14 December 2015; published 8 January 2016)

Optical pumping can increase the polarization of nuclear spins in semiconductors, such as GaAs, by many orders of magnitude, improving the sensitivity in conventionally detected nuclear magnetic resonance (NMR) experiments. Optical detection of these NMR transitions may further increase the sensitivity, allowing an all-optical NMR which is free of radio-frequency fields. Here we report all-optical NMR experiments in a $GaAs/Al_{0.35}Ga_{0.65}As$ two-dimensional electron system. We observed multiple magnetic resonance of nuclear species in the sample when the modulation frequency of the pump light was $\frac{1}{2m+1}$ of the fundamental NMR frequency (multiple NMR), where m is an integer. Such multiple NMRs arise from interaction between modulated spins of polarized electrons and nuclear spins.

DOI: 10.1103/PhysRevB.93.035302

I. INTRODUCTION

Nuclear magnetic resonance (NMR) with high sensitivity is a powerful tool to study nuclear spin physics in semiconductors [1]. Recent progress in quantum information processing requires a deep understanding of nuclear spins, which are almost ideal qubits for the manipulation and storage of quantum information [2,3], especially in semiconductor quantum structures where the nuclear properties may vary on mesoscopic scales. In semiconductor NMR experiments, dynamic nuclear polarization (DNP) via hyperfine interaction with spin-polarized electrons allows accessing the nuclear spins at much higher temperatures and much weaker magnetic fields [4–6], however, there remain plenty of technical difficulties to reach extremely high sensitivity and spatial resolution for feasible quantum information processing.

Optically detected NMR (ODNMR) was a great step towards this direction where the resonant effect of the nuclear spins on electron spin polarization via hyperfine interaction can be measured through the polarization of photoluminescence [7–12] or Faraday/Kerr rotation [4,5,13]. This technology has been extended from bulk semiconductors to semiconductor quantum wells [14–20] and quantum dots [21,22] with much less nuclear spins contributing to the signal. Several kinds of resonance have been observed under ODNMR conditions, for example, fundamental resonances [16,19,23–29], mixed resonances [26,27], second harmonics [24–27], and half-harmonics [26,27,30,31].

On the basis of ODNMR, the Awschalom Group carried out an all-optical NMR [32–34] with the time-resolved Faraday/Kerr rotation technique. This technique is free of radio-frequency fields since the electron spin excitation by a periodic optical pulse train not only prepares a hyperpolarized nuclear moment, but also destroys it resonantly in a suitable magnetic field which is proportional to the pulse frequency, thus opening a door to study the complex electron-nuclei spin interaction.

Here, we report an all-optical NMR measurement in a GaAs/AlGaAs two-dimensional electron system (2DES). We modulated the pump light by an acousto-optical modulator (AOM) and detected the NMR signal versus modulation frequency of the pump light in a fixed external magnetic field. Interestingly, lots of peaks (or dips) appear when the modulation frequency equals $\frac{f_\alpha}{2m+1}$, where f_α is the fundamental NMR frequency of nuclear species α and m is an integer. We ascribe such multiple NMR signals to electron-nuclei spin interaction.

II. SAMPLE STRUCTURE AND EXPERIMENTAL SETUP

Our sample was a 2DES embedded in a GaAs/AlGaAs heterostructure grown by molecular beam epitaxy on a (001)-oriented semi-insulating substrate as shown in Fig. 1(a). A 1400-nm GaAs buffer layer was first grown on the substrate followed by a 90-nm undoped $Al_{0.35}Ga_{0.65}As$ spacer layer, a 14-nm Si-doped ($3.1 \times 10^{18}\,cm^{-3}$) $Al_{0.35}Ga_{0.65}As$ layer, a 10-nm undoped AlGaAs barrier layer, and finally a 7-nm GaAs cap layer. The 2DES sample was mounted inside a vibration-free optical cryostat with a tunable temperature from 6.5 to 300 K. An electromagnet provided a small transverse magnetic field up to 750 G.

We used a time-resolved Kerr rotation (TRKR) system to carry out the all-optical NMR measurements. A mode-locked Ti:sapphire laser gave the pump and the probe beams with 150-fs pulse trains at an 80-MHz repetition rate. The right σ^+ or left σ^- circularly polarized pump light and the time-delayed linearly polarized probe light were focused to spatially overlap onto the sample with a diameter of 100 μm and an angular separation of 4°. The pump light intensities were modulated by AOM, which was controlled by a function generator. The modulation frequency range could be tuned from 0 to 100 kHz. Such a modulated circularly polarized pump light played the roles of both Overhauser DNP and radio-frequency fields [32]. The Kerr rotation angle was detected by a balanced photoreceiver and a lock-in amplifier. It revealed the dynamics of electron spins and thus the nuclear spin dynamics as they affect each other through Knight interaction [4].

The photon energy of the pump light was fixed at 1.516 eV, which corresponds to the resonance optical transition energy of a ground state in 2DES at 7 K. The sample was intentionally shined with a laser during the cooling process, which allowed a much longer spin dephasing time (up to 4 ns) than that

*Corresponding author: jiyang@semi.ac.cn

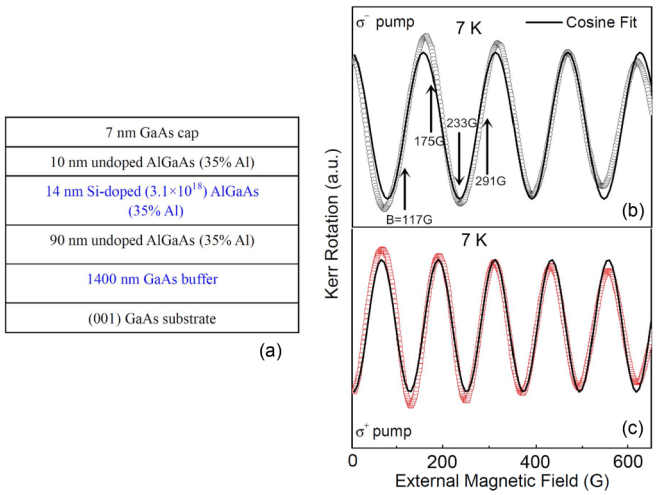

FIG. 1. (a) Sample structure. (b) Black circles and (c) red open squares show the Kerr rotation signals at 7 K induced by σ^-- and σ^+-polarized optical excitations, respectively. They were measured while probe pulse arrival time was fixed at a small negative delay (~ -67 ps) prior to the pump pulse. The solid lines are cosine fits, and the different periods are evidence of nuclear magnetic fields. The following experiments were carried out at different external magnetic fields $B_{\text{ext}} = 117$, 175, 233, and 291 G as indicated by arrows in (b).

in our previous works (about 1 ns) [35,36]. The long spin dephasing time of the electrons enhanced the DNP via contact hyperfine coupling. In this experimental setup, we could see all-optical NMR signals for ^{69}Ga, ^{71}Ga, ^{75}As, and ^{27}Al [37], whose gyromagnetic ratios (spin) are 2.0108 (3/2), 2.5549 (3/2), 1.4349 (3/2), and 2.1829 (5/2), respectively.

III. RESULTS AND DISCUSSIONS

First we measured Kerr rotation signals versus external magnetic fields at a fixed time delay ($\Delta t \sim 12.433$ ns). For the following NMR experiments, optical excitation was always on, and DNP gets saturated prior to the measurements. The temperature was 7 K, pump (probe) intensity was 8 mW (0.8 mW), and the modulation frequency of the pump light was 13.33 kHz. As shown in Figs. 1(b) and 1(c), the black circles and red open squares are the Kerr rotation signals induced by σ^- and σ^+ pump lights, respectively. The Kerr rotation signals have different periods between 0 and 650 G, which are 4.14 and 5.28 for σ^- and σ^+ pump lights. As the oscillating part of the Kerr rotation signal could be expressed as $\theta_K = \cos(\mu_g g B_{\text{tot}} \Delta t/\hbar + \varphi)$, where B_{tot} includes the external magnetic field and the nuclear magnetic field, so this difference in periods comes from a polarization-dependent nuclear magnetic field caused by DNP via electron-nuclei spin hyperfine interaction. So, we have successfully detected electron spin dynamics and coupled electron-nuclei spin dynamics in a local area of the laser spot size. Furthermore, the fitting results in Figs. 1(b) and 1(c) suggest that the nuclear magnetic field is about 80 G and the g factor is 0.417, being consistent with the g factor of 2DES in Ref. [35].

In the all-optical NMR measurements, we swept the modulation frequency of the σ^- pump beam intensity f_{mod} with a slow rate (10 Hz s) by controlling AOM via a function

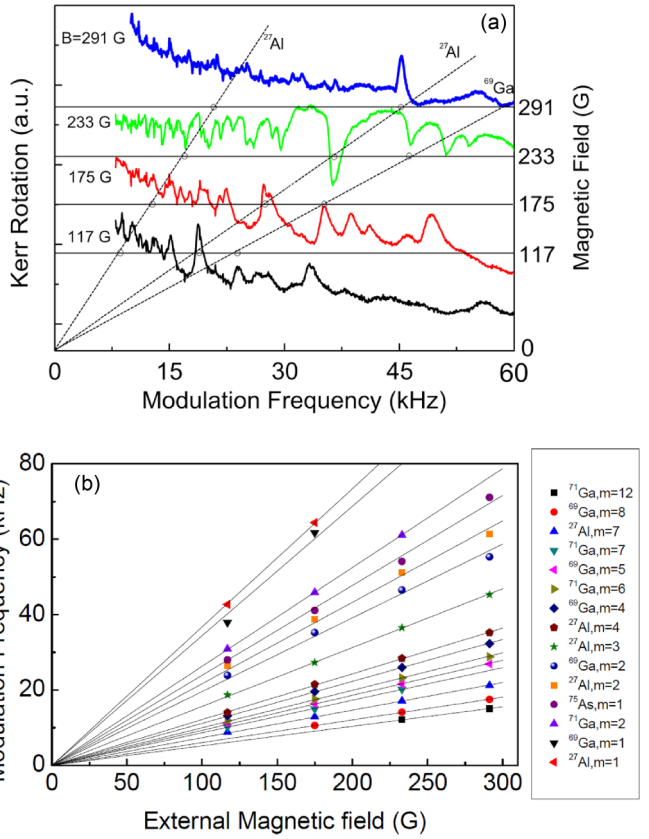

FIG. 2. (a) Kerr rotation versus modulation frequency at external magnetic fields $B_{\text{ext}} = 117$ G (black line), 175 G (red line), 233 G (green line), and 291 G (blue line), respectively. A lot of peaks and dips can be seen. To give a better show, the curves have been shifted vertically with a certain constant. The solid lines indicate four magnetic fields, and some representative peaks and dips are indicated by the open circles. The dashed lines are guides to the eyes. (b) Modulation frequency as a function of external magnetic fields shows multiple resonance at fields proportional to the modulation frequency. The solid lines are linear fits. All of these resonances occur at $f_\alpha/(2m+1)$ of ^{69}Ga, ^{71}Ga, ^{75}As, and ^{27}Al for different m's.

generator. Figure 2(a) shows the time-domain signal of the probe beam for the cases of the external magnetic field $B_{\text{ext}} = 117$, 175, 233, and 291 G, respectively. There are lots of peaks and dips [38] on the curves, and their positions are far away from the fundamental NMR range for any isotope species in our sample. In order to figure out the physical meaning of these peaks (or dips), especially whether they have a certain relationship with fundamental NMR, we compared the gyromagnetic ratio (γ) of these observed signals with that of the fundamental NMR of all isotope species in our sample, say, ^{69}Ga, ^{71}Ga, ^{75}As, and ^{27}Al, respectively. It turns out that most of the γ values equal $\frac{1}{2m+1}$ for certain isotope species. Because of the noisy background, observed peaks will inevitably contain noise, and noise does not shift linearly with external magnetic fields. So, peaks identified as resonances have to meet two conditions: (a) The frequency of the peaks must be $\frac{1}{2m+1}$ for the fundamental NMR of either isotope species. (b) These peaks must move linearly with magnetic fields. Some representative peaks and dips at different B_{ext}'s are shown in Fig. 2(a). They form straight

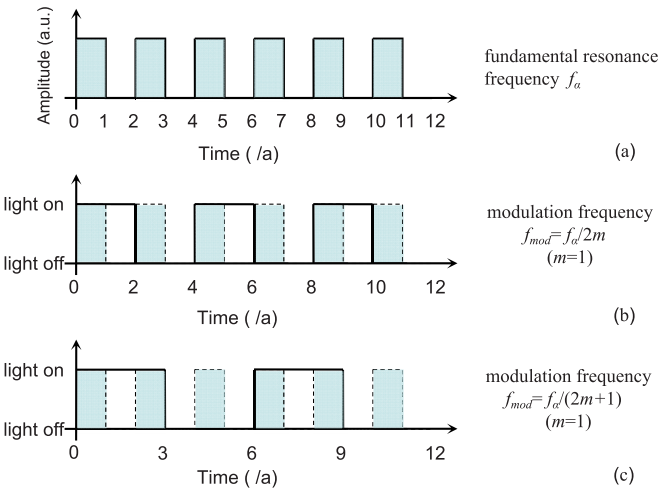

FIG. 3. A physical picture of the multiple resonance condition. (a) The fundamental resonance of isotope species α is expressed by a square-wave sequence with frequency $f_\alpha = \frac{1}{2a}$. (b) Pump light intensity is modulated with frequency $f_{\rm mod} = f_\alpha/2$ (it also works for $f_{\rm mod} = f_\alpha/2m$). The first half cycle ($0 \rightarrow 2$, light on) and the second half cycle ($2 \rightarrow 4$, light off) contain same high levels and low levels of fundamental resonance. (c) Pump light intensity is modulated with frequency $f_{\rm mod} = f_\alpha/3$ [it also works for $f_{\rm mod} = f_\alpha/(2m+1)$], the first half cycle ($0 \rightarrow 3$, light on) contains two high levels and one low level whereas the second half cycle ($3 \rightarrow 6$, light off) contains one high level and two low levels, and the nuclei systems could be effectively modulated at this time.

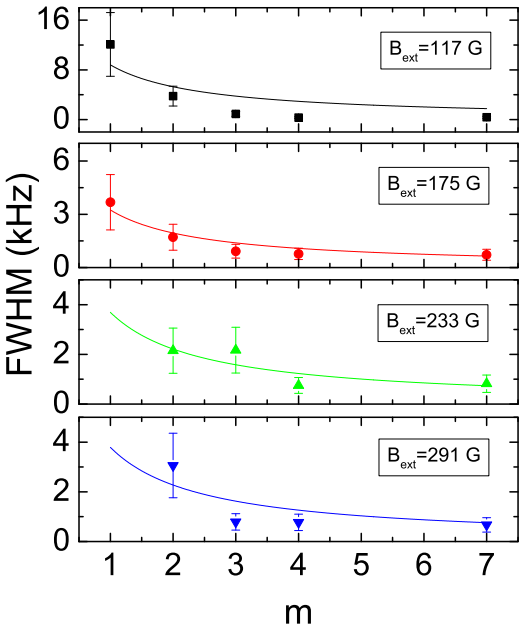

FIG. 4. The FWHM of the ^{27}Al's multiple resonance signals as a function of m at external magnetic fields $B_{\rm ext} = 117$, 175, 233, and 291 G, respectively. They are fitted with Eq. (3) (solid lines), and the nominal nuclear spin dephasing time of ^{27}Al is identified as about 40 μs.

lines, going through the origin. It is not difficult to identify the resonances in the middle and right dashed lines, but the identification of the resonance at 21.2 kHz when $B = 291$ G is not so straightforward because of the noisy background. Because it meets the conditions (a) ($m = 7$ for ^{27}Al) and has been confirmed by the data of the other magnetic fields, that is, peaks at $B_{\rm ext} = 117$, 175, and 233 G on the left dashed line, it is thus identified as a resonance signal. Those peaks that do not meet the above conditions are given up. The position of the peaks identified as resonances at different $B_{\rm ext}$'s are shown in Fig. 2(b), and they could be fitted perfectly by straight lines through the origin with the biggest difference being less than 5% for all experimental points. So, the relation between $f_{\rm mod}$ and f_α could be expressed as $f_{\rm mod} = \frac{f_\alpha}{2m+1}$, which we call the multiple magnetic resonance condition. Note that there are many missing peaks (or dips) for the multiple magnetic resonance and we have only observed $m = 1$ for ^{75}As, $m = 2$, 6, 7, 12 for ^{71}Ga, $m = 1$, 2, 4, 5, 8 for ^{69}Ga, and $m = 1$, 2, 3, 4, 7 for ^{27}Al.

Figure 3 shows a physical picture of the multiple resonance condition. The fundamental resonance of isotope species α is expressed by a square-wave sequence with frequency $f_\alpha = \frac{1}{2a}$, where a is an arbitrary constant, the high levels of this square-wave sequence are filled in blue as shown in Fig. 3(a). The modulation frequency of pump beam intensity $f_{\rm mod}$ could be expressed by the other square-wave sequences with $f_{\rm mod} = \frac{f_\alpha}{2m}$ or $f_{\rm mod} = \frac{f_\alpha}{2m+1}$. For the sake of simplicity, we set $m = 1$ when we compare these two cases, and the results can apply to the cases with any integer m. When $f_{\rm mod} = f_\alpha/2$ [Fig. 3(b)], the first half cycle ($0 \rightarrow 2$, light on) and the second half cycle ($2 \rightarrow 4$, light off) contain same high levels and low levels of fundamental resonance, so the nuclei systems will not respond to this modulation frequency, in other words, the contributions from the two half cycles are the same, and a lock-in measurement cannot see any difference. The case is quite different for $f_{\rm mod} = f_\alpha/3$ [Fig. 3(c)] where the first half cycle ($0 \rightarrow 3$, light on) contains two high levels and one low level whereas the second half cycle ($3 \rightarrow 6$, light off) contains one high level and two low levels, meaning that the nuclei systems could be effectively modulated when $f_{\rm mod} = \frac{f_\alpha}{2m+1}$ and multiple magnetic resonance has occurred.

Such a simple picture may be described in more mathematical detail with the following assumptions. The first assumption is $\tau_e \ll t_1 \ll t_2 \ll \tau_n$, where τ_e and τ_n are the dephasing time T_2^* of the electron spin and the nuclear spin, respectively. t_1 is the time interval between successive pulses of the femtosecond laser, and t_2 is the square-wave chopping period of the pump laser. The typical values of t_1 and t_2 are 12.5 ns and 10 μs. The Larmor frequency of electron spin ω_e is much larger than that of nuclear spin ω_n. The second assumption is that there is a weak coupling between the electron spin and the nuclear spin, through which the electron spin (a net spin is optically generated via the pump laser with circular polarization) could be transferred to nuclei. It is described with a nominal coupling coefficient α. The TRKR measurement system has the following arrangement: The z axis points to the direction of the pump laser, the y axis points to the direction of the transverse magnetic field, and x, y, z together make a right-handed coordinate system. With all the assumptions outlined above, we find that a net nuclear spin at the multiple resonance (as a function of time) goes as follows

(see the Supplemental Material [39]):

$$S_{nx} \approx A\cos(\omega_n t + \gamma),$$
$$S_{nz} \approx A\sin(\omega_n t + \gamma), \tag{1}$$

with

$$\begin{aligned} A &= \alpha A_1 A_2 A_3 \\ &= \alpha s_0 \frac{1}{\sqrt{(\omega_e t_e)^2 + 1}} \frac{t_e}{t_1} \frac{1}{\sqrt{(\omega_n \tau_n)^2 + 1}} \\ &\quad \times \frac{t_2}{t_1} \frac{1}{\sqrt{[(2m+1)\delta\omega\tau_n]^2 + 1}} \frac{\tau_n}{t_2}, \\ \gamma &= \gamma_1 + \gamma_2 + \gamma_3 \\ &= \arctan[\omega_e \tau_e] \\ &\quad + \arctan[\omega_n \tau_n] + \arctan[(2m+1)\delta\omega\tau_n], \end{aligned} \tag{2}$$

where $\delta\omega = \omega_2 - \omega_m$ with $\omega_2 \equiv 2\pi/t_2 = 2\pi f_{\text{mod}}$ and $\omega_m \equiv \omega_n/(2m+1)$ for any integer m. A_1 and γ_1 describe the transfer of the electron spin to the nuclei; A_2 and γ_2 describe the accumulation of nuclear spin in one pump period; A_3 and γ_3 describe the multiple resonance condition. Thus, it is easy to see that the net nuclear spin becomes significant if and only if $(2m+1)\delta\omega\tau_n \ll 1$, which means the signal reaches peak values when $f_{\text{mod}} = \frac{f_\alpha}{2m+1}$ with a full width at half maximum (FWHM),

$$\delta f = \frac{1}{\tau_n(2m+1)}. \tag{3}$$

Considering the number of resonance signals as well as signal strength, the FWHM of the ^{27}Al's resonances at different integer m's was studied at external magnetic fields $B_{\text{ext}} = 117$, 175, 233, and 291 G. The results are shown in Fig. 4. Larger error bars were obtained when m was small. The reason is that the peaks located in the high-frequency range for small m and the frequency of the pump light are controlled by AOM, whose response is no longer a good square wave at high frequencies. All the data except $B_{\text{ext}} = 117$ G can be fitted well by Eq. (3). The fitting results are shown in Fig. 4 by lines, and we obtain τ_n for ^{27}Al of about 40 μs. This value is smaller by four to five orders of magnitude than that of traditional NMR [1] as electron-nuclei spin interaction is the key factor in all-optical NMR and τ_n measured here is strongly limited by the electron spin dephasing time.

IV. CONCLUSIONS

Strong interaction between nuclear spins and electron spins gives rise to a rich spectrum of all-optical NMR for the three spin- 3/2 nuclei and spin- 5/2 nuclei in the AlGaAs barrier. By scanning the intensity modulation frequency of circularly polarized pump light with AOM, we observed multiple nuclear magnetic resonance at $\frac{f_\alpha}{2m+1}$, which could give us more information to understand the electron-nuclei spin physics.

ACKNOWLEDGMENTS

This work has been financially supported by the NSFC under Grants No. 11404325 and No. 91321310 and the National Basic Research Program of China under Grant No. 2013CB922304.

[1] A. Abragam, *The Principles of Nuclear Magnetism* (Oxford University Press, Oxford, 1961).
[2] M. A. Nielson and I. L. Chuang, *Quantum Computation and Quantum Information* (Cambridge University Press, Cambridge, UK, 2002).
[3] D. D. Awschalom, D. Loss, and N. Samarth, *Semiconductor Spintronics and Quantum Computation* (Springer-Verlag, Berlin, 2002).
[4] F. Meier and B. P. Zakharchenya, *Optical Orientation* (North-Holland, New York, 1984).
[5] *Spin Physics in Semiconductors*, edited by M. I. Dyakonov (Springer-Verlag, Berlin, 2008).
[6] S. E. Hayes, S. Mui, and K. Ramaswamy, J. Chem. Phys. **128**, 052203 (2008).
[7] A. I. Ekimov and V. I. Safarov, Pis'ma Zh. Eksp. Teor. Fiz. **15**, 453 (1972) [Sov. Phys. JETP **15**, 179 (1972)].
[8] V. L. Berkovits, A. I. Ekimov, and V. I. Safarov, Zh. Eksp. Teor. Fiz. **65**, 346 (1973) [Sov. Phys. JETP **38**, 169 (1974)].
[9] M. I. Dyakonov, V. I. Perel, V. L. Berkovits, and V. I. Safarov, Zh. Eksp. Teor. Fiz. **67**, 1912 (1974) [Sov. Phys. JETP **40**, 950 (1975)].
[10] D. Paget, Phys. Rev. B **24**, 3776 (1981).
[11] V. K. Kalevich and V. G. Fleisher, Izv. Akad. Nauk SSSR, Ser. Fiz. **47**, 2294 (1983) [Bull. Acad. Sci. USSR Phys. Ser. **47**, 5 (1983)].
[12] M. Eickhoff, B. Lenzman, G. Flinn, and D. Suter, Phys. Rev. B **65**, 125301 (2002).
[13] T. A. Kennedy, J. Whitaker, A. Shabaev, A. S. Bracker, and D. Gammon, Phys. Rev. B **74**, 161201(R) (2006).
[14] V. K. Kalevich, V. L. Korenev, and O. M. Fedorova, Pis'ma Zh. Eksp. Teor. Fiz. **52**, 964 (1990) [JETP Lett. **52**, 349 (1990)].
[15] G. P. Flinn, R. T. Harley, M. J. Snelling, A. C. Tropper, and T. M. Kerr, J. Lumin. **45**, 218 (1990).
[16] M. Eickhoff, B. Lenzmann, D. Suter, S. E. Hayes, and A. D. Wieck, Phys. Rev. B **67**, 085308 (2003).
[17] M. Eickhoff and D. Suter, J. Magn. Reson. **166**, 69 (2004).
[18] M. Poggio and D. D. Awschalom, Appl. Phys. Lett. **86**, 182103 (2005).
[19] H. Sanada, Y. Kondo, S. Matsuzaka, K. Morita, C. Y. Hu, Y. Ohno, and H. Ohno, Phys. Rev. Lett. **96**, 067602 (2006).
[20] Y. Kondo, M. Ono, S. Matsuzaka, K. Morita, H. Sanada, Y. Ohno, and H. Ohno, Phys. Rev. Lett. **101**, 207601 (2008).
[21] D. Gammon, S. W. Brown, E. S. Snow, T. A. Kennedy, D. S. Katzer, and D. Park, Science **277**, 85 (1997).
[22] B. Urbaszek, X. Marie, T. Amand, O. Krebs, P. Voisin, P. Maletinsky, A. Högele, and A. Imamoglu, Rev. Mod. Phys. **85**, 79 (2013).
[23] D. Paget, G. Lampel, and B. Sapoval, Phys. Rev. B **15**, 5780 (1977).

[24] V. K. Kalevich, V. D. Kul'kov, I. A. Merkulov, and V. G. Fleisher, Sov. Phys.-Solid State **24**, 1195 (1982).
[25] S. K. Buratto, J. Y. Hwang, N. D. Kurur, D. N. Shykind, and D. P. Weitekamp, Bull. Magn. Reson. **15**, 190 (1993).
[26] J. Strand, X. Lou, C. Adelmann, B. D. Schultz, A. F. Isakovic, C. J. Palmstrøm, and P. A. Crowell, Phys. Rev. B **72**, 155308 (2005).
[27] Y. S. Chen, D. Reuter, A. D. Wieck, and G. Bacher, Phys. Rev. Lett. **107**, 167601 (2011).
[28] M. N. Makhonin, E. A. Chekhovich, P. Senellart, A. Lemaitre, M. S. Skolnick, and A. I. Tartakovskii, Phys. Rev. B **82**, 161309(R) (2010).
[29] E. A. Zhukov, A. Greilich, D. R. Yakovlev, K. V. Kavokin, I. A. Yugova, O. A. Yugov, D. Suter, G. Karczewski, T. Wojtowicz, J. Kossut, V. V. Petrov, Y. K. Dolgikh, A. Pawlis, and M. Bayer, Phys. Rev. B **90**, 085311 (2014).
[30] V. L. Berkovits and V. I. Safarov, Pis'ma Zh. Eksp. Teor. Fiz. **26**, 377 (1977) [JETP Lett. **26**, 256 (1977)].
[31] P. T. Eles and C. A. Michal, Prog. Nucl. Magn. Reson. Spectrosc. **56**, 232 (2010).
[32] J. M. Kikkawa and D. D. Awschalom, Science **287**, 473 (2000).
[33] G. Salis, D. T. Fuchs, J. M. Kikkawa, D. D. Awschalom, Y. Ohno and H. Ohno, Phys. Rev. Lett. **86**, 2677 (2001).
[34] G. Salis, D. D. Awschalom, Y. Ohno and H. Ohno, Phys. Rev. B **64**, 195304 (2001).
[35] X. Z. Ruan, H. H. Luo, Y. Ji, Z. Y. Xu and V. Umansky, Phys. Rev. B **77**, 193307 (2008).
[36] H. H Luo, X. Qian, X. Z. Ruan, Y. Ji and V. Umansky, Phys. Rev. B **80**, 193301 (2009).
[37] Because the wave function of 2DES partially penetrates into the potential barrier AlGaAs, we could expect to see an all-optical NMR signal of Al, however, these signals for Al in our experimental results are much stronger than what would be expected, and the reason is unclear yet.
[38] In Fig. 1, the oscillating parts of the Kerr rotation signals are shown as cosine functions of the magnetic fields. In order to obtain large resonance signals, we try to perform experiments in the external magnetic fields located at about the antinodes of the cosine function [indicated by arrows in Fig. 1(b)]. Resonance signals in peaks or dips are not only related to the external magnetic fields, but also to the changes in nuclear magnetic fields when resonances occur, which we cannot accurately obtain yet.
[39] See Supplemental Material at http://link.aps.org/supplemental/10.1103/PhysRevB.93.035302 for mathematical detail of multiple NMR.